ELSEVIER

International Journal of Mass Spectrometry 206 (2001) 27–43

International Journal of Mass Spectrometry

Effective potential and the ion axial beat motion near the boundary of the first stable region in a nonlinear ion trap

M. Sudakov*

Department of General Physics, Ryazan State Pedagogical University, Svoboda St. 46, Ryazan, Russia, 390000

Received 21 August 2000; accepted 20 September 2000

Abstract

Small higher-order field imperfections of the main trapping quadrupole field are well known to have a strong influence on the performance of modern quadrupole mass spectrometers. Mass selectivity is usually achieved by means of the stability region boundaries. The stability diagram for ion motion is the area on the plane of voltage parameters for which the quadrupole field is able to trap ions of a given mass. Hence, the trapping efficiency of the quadrupole field is equal to zero at a boundary of the stability region. In this case, the trapping properties of the RF field depend on higher field imperfections regardless of how small they are compared to the quadrupole field. The ion motion with parameters close to the boundary $\beta_z = 1$ is investigated in this article. The influence of nonlinear field imperfections is taken into account. A treatment similar to trajectory averaging in a pseudopotential is possible in this case. The ion motion has the characteristics of a beat with a fast oscillation at half the frequency of the RF and a slowly varying envelope. The ion motion is described by a dynamic equation for the envelope. This equation has the form of a Newton equation for the motion of a particle in a potential field. The effective potential function of the envelope is derived and investigated. The effective potential well is rather different for the cases of negative and positive even-order higher fields. The results are applied to the mass-selective axial instability scan of an ion trap. The influence of negative higher field harmonics explains the ejection delay and poor mass resolution of the Paul trap with truncated electrodes. Positive even-field imperfections are shown to be beneficial to the mass selective axial instability scan. This explains why stretched or hyperbolic angle modified traps give improved performance. Stable ion motion outside of the first stable region is predicted. This motion has the character of a limit cycle, and all ions move coherently in the radio frequency field. (Int J Mass Spectrom 206 (2001) 27–43) © 2001 Elsevier Science B.V.

Keywords: Stretched trap; Envelope equation; Effective potential; Mass selective scan; Limit cycle

1. Introduction

The use of the quadrupole ion trap has been based on the discovery of the mass-selective axial instability ejection [1], pioneered commercially by Finnigan MAT. In this method, the amplitude of the radio frequency (RF) trapping potential is ramped so as to render unstable axially and sequentially the trajectories of ions of different mass to charge ratios at the $\beta_z = 1$ boundary of the stability diagram. The most recent commercial ion traps do not use mass selective instability scan exactly. Instead they use selective dipole excitation with a frequency different from the main trapping RF. In this case ejection happens at lower β values. In fact, almost all commercial instruments do not use the pure quadrupole electrode

* E-mail: Sudakov@qms.sotcom.ru

PII S1387-3806(00)00380-8

geometry arrangement of a trap. In the Finnigan ion trap, the separation of the end-cap electrodes was stretched [2] by ~11%, and the Bruker-Franzen Analytic GmbH instruments use an ion trap with a modified hyperbolic angle geometry [3]. The physical requirements of a real ion trap also introduce deviations from ideality such that the field within the ion trap is no longer linear. These deviations have been called field faults and can be described by the superposition of higher-order multipole fields that give nonlinear electric fields (a nonlinear trap).

In a series of papers [4–7], Y. Wang, J. Franzen, and K. P. Wanczek calculated the multipole field composition [5], developed the theory of nonlinear resonances [4], and developed methods of modeling of ion axial motion [7] for traps with higher multipole fields. It was found that in a Paul trap, a small negative higher field component is present because of the electrode truncation. In contrast to this, an ion trap with a stretched geometry has a positive octopole field. By means of computer trajectory simulations, Franzen investigated the boundary mass-selective ion ejection in a nonlinear ion trap [6]. His calculations showed that there is an ion ejection delay when a negative octopole field is present. He also explained the constructive role of a positive octopole field in this protocol of ion trap operation.

It was noted in the early experiments with the Paul ion trap, that the mass/charge ratios of some ions were incorrectly assigned. This chemical mass shift was as much as 0.7 Th. This problem was also solved by changing the axial dimension between the end-cap electrodes and the center of the ion trap. Recent investigations of this problem [8,9] reveal that there are two main reasons of chemical mass shifts: 1) compound-dependent fragmentation at the last oscillations so that in fact fragments are ejected ahead of parent ion; 2) mass-dependent re-distribution of ions due to space charge. The ejection delay caused by the influence of higher fields increase these shifts. The holes in the end-cap electrodes cause much stronger negative higher fields than the truncation of the electrodes. In the ion trap of stretched geometry, positive higher fields are introduced deliberately to overcome the influence of such field faults. Until now, the influence of high-order field imperfections on the ion motion has been studied only by computer simulation.

This article is a theoretical treatment of the ion motion with parameters close to the stability boundary $\beta_z = 1$. Here the ion axial motion has a beat-like character with a slowly varying envelope. In this case, a theoretical treatment similar to the averaged motion in a pseudopotential [10,11,12], as is used for low q values, is possible. A dynamic equation for the beat envelope is derived. This envelope equation has the form of a Newton equation of motion for a particle in a potential field. It is evident from this equation that at the boundary of the stable region the quadrupole term in the trapping pseudopotential is zero. Hence, the trapping properties of the field depend strongly on higher field imperfections. Thus, the strong influence of small higher field imperfections on the operation of quadrupole devices is explained.

The article is organized as follows: The first section is devoted to a description of the electric field of an axially symmetric ion trap with higher-order multipoles. The equation of ion axial motion in an oscillating potential is then derived. The frequency spectrum and other properties of the ion motion near the $\beta_z = 1$ boundary are described. The second section discusses the equations of the first-order beat envelope of the ion motion with an octopole field. The derivations of the higher-order equation of the beat envelope and of the equation with hexapole and higher fields are given in appendices A and B. Results of the beat-envelope equation without field imperfections are also described. The effective potential function of the envelope is discussed. The third section describes the results of the beat-envelope equation for the case where small higher-order fields are present in the trapping quadrupole field. The stability conditions of the ion motion are investigated. The approximate solutions of the beat-envelope equation are verified by the direct numerical solution of the ion-motion equation. The properties of the effective potential function are described in detail for the cases of positive and negative higher multipoles. The result is applied to the description of the ion ejection in a

boundary mass-selective scan. A discussion of the results and perspectives of the beat-envelope equation form the last section of this article.

2. Equation of ion motion in a nonlinear ion trap

2.1. Electric field of a nonlinear ion trap

The electric potential near the center of an ion trap with axially symmetrical electrodes may be expressed in spherical coordinates (ρ, ϕ, θ) as an infinite series of orthogonal functions, each of which is the solution of Laplace's equation:

$$\Phi(\rho, \varphi, \theta) = -(U + V\cos\Omega t) \times \left[A_0 + \sum_{N=2}^{\infty} A_N \left(\frac{\rho}{r_0}\right)^N P_N(\cos\theta) \right]. \quad (1)$$

Here, V and Ω are the amplitude (0-peak) and angular frequency of the trapping RF voltage, U is the DC voltage of the ring electrode, P_N are Legendre polynomials, r_0 is the ring electrode radius, and A_N are dimensionless weight factors of the field harmonics ($A_1 = 0$, because the dipole field is assumed to be zero). The field harmonics can be expressed in cylindrical coordinates (z, r, ϕ), as follows:

$$\rho^2 P_2(\cos\theta) = \tfrac{1}{2}(2z^2 - r^2) \quad \text{(quadrupole)},$$

$$\rho^3 P_3(\cos\theta) = \tfrac{1}{2}(2z^3 - 3zr^2) \quad \text{(hexapole)},$$

$$\rho^4 P_4(\cos\theta) = \tfrac{1}{8}(8z^4 - 24z^2r^2 + 3r^4) \quad \text{(octopole)},$$

$$\rho^5 P_5(\cos\theta) = \tfrac{1}{8}(8z^5 - 40z^3r^2 + 15zr^4) \quad \text{(decapole)},$$

$$\rho^6 P_6(\cos\theta) = \tfrac{1}{16}(16z^6 - 120z^4r^2 + 90z^2r^4 - 5r^6) \quad \text{(dodecapole)}.$$

A pure quadrupole field where the RF is applied to the ring electrode only will have $A_2 = 1$, $A_0 = -0.5$, $A_3 = A_4 = \ldots = 0$.

The equation of axial motion for an ion with mass M and charge e in the electric field with the potential of Eq. (1) will be

$$M\frac{d^2z}{dt^2} + 2e\frac{A_2}{r_0^2}(U + V\cos\Omega t)\cdot z = -e(U + V\cos\Omega t)\cdot\frac{\partial}{\partial z}\sum_{N>2} A_N P_N(\cos\theta)\frac{\rho^N}{r_0^N} \quad (2)$$

Helium gas at a pressure of 0.1 to 1.0 mTorr is used in commercial ion traps for collisional damping of ion oscillations. Damping is not included in Eq. (2) but is included in the trajectory calculations in section 4. The amplitudes of the axial oscillations increase during boundary ejection, while the radial motion remains stable. Under these conditions, a good approach to the description of motion in the z direction is to neglect the radial motion and set $r = 0$. This brings us to the Z-axis simulation model described by Franzen [6], which cannot simulate effects that involve motion in the r direction. However, the mass-selective instability scan with its ion ejection in the z direction at the boundary $\beta_z = 1$ is ideally suited to this type of simulation.

For the case where there is an RF-only trapping voltage, $U = 0$ and Eq. (2) may be expressed in dimensionless units as follows:

$$\frac{d^2u}{d\xi^2} + 2q\cos(2\xi)\times u = -q\cos(2\xi) \times \sum_{N>2} N\alpha_N u^{N-1}. \quad (3)$$

$$\xi = \frac{\Omega t}{2}, \qquad u = \frac{z}{z_0}, \qquad q = \frac{4eA_2V}{Mr_0^2\Omega^2},$$

$$\alpha_N = \frac{A_N}{A_2}\times\left(\frac{z_0}{r_0}\right)^{N-2}.$$

Here, $2z_0$ is the distance between the end-cap electrodes. The dimensionless parameter α_N is the amplitude of the Nth field harmonic in comparison to the quadrupole field.

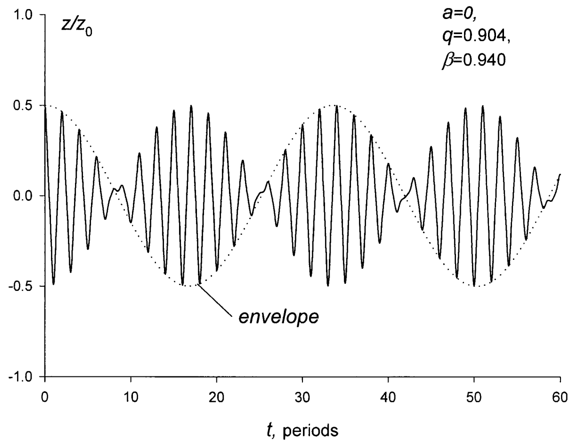

Fig. 1. Ion axial oscillations with initial conditions: $z(0) = 0.5 \times z_0$; $z'(0) = 0$. The parameters of the ion motion are close to the boundary of the stable region. The Z-axis is scaled in units of z_0, the time scale is in periods of RF.

2.2. Beat motion in the mass-selective axial instability scan

The linear Mathieu equation (Eq. [3] with $\alpha_N = 0$) gives stable motion in the region from $q = 0$ (the $\beta_z = 0$ boundary) up to $q_0 = 0.908047$ (the $\beta_z = 1$ boundary). The dimensionless parameter q is inversely proportional to the ion mass. Therefore, for a given starting RF amplitude $V_{\min}$, all ions with mass greater than

$$M_{\min} = \frac{4eA_2V_{\min}}{q_0 r_0^2 \Omega^2} \tag{4}$$

are trapped. After this ion storage period, the amplitude of the RF voltage is ramped to achieve an analytical mass scan. During this period, ions of different mass to charge ratios, M/e, meet the $\beta_z = 1$ boundary sequentially, become unstable, and are ejected through holes in the end-cap electrode to a detector. Hence, understanding of the influence of field faults on boundary ejection may be achieved by the investigation of the ion motion near the $\beta_z = 1$ boundary of the stability region.

Direct numerical calculation of the ion trajectories shows that the ion motion has the characteristics of a beat, with a slowly varying envelope (Fig. 1). The frequency spectrum of the linear Mathieu equation [13] shows that when $\beta \sim 1$ and $\beta < 1$, the spectrum consists of pairs of harmonics with approximately equal amplitudes. The frequencies of pairs are also almost equal and are given by

$$\omega_n^+ = \Omega \times |n + 0.5\beta| \quad \text{and} \quad \omega_n^- = \Omega \times |n + 1 - 0.5\beta|, \quad n = 0, 1, 2, \ldots . \tag{5}$$

The part of the ion oscillation that is described by these two harmonics can be written as

$$\begin{aligned} C_n \cos \omega_n^+ t + C_n \cos \omega_n^- t &= 2C_n \cos\left(\frac{\omega_n^- - \omega_n^+}{2} t\right) \cos\left(\frac{\omega_n^- + \omega_n^+}{2} t\right) \\ &= 2C_n \cos\left(\frac{\omega_n^- - \omega_n^+}{2} t\right) \cos\left(\frac{\omega_n^- + \omega_n^+}{2} t\right) \\ &= 2C_n \cos\left(\frac{\omega_n^- - \omega_n^+}{2} t\right) \cos\left(\frac{\omega_n^- + \omega_n^+}{2} t\right) \\ &= 2C_n \cos\left(\frac{\omega_n^- - \omega_n^+}{2} t\right) \cos\left(\frac{\omega_n^- + \omega_n^+}{2} t\right) \\ &= 2C_n \cos\left(\frac{\omega_n^- - \omega_n^+}{2} t\right) \cos\left(\frac{\omega_n^- + \omega_n^+}{2} t\right) \\ &= 2C_n \cos\left(\frac{1 - \beta}{2} \Omega t\right) \cos\left(\frac{n + 1}{2} \Omega t\right). \end{aligned} \tag{6}$$

The frequency difference $\omega_n^- - \omega_n^+$ does not depend on n. Eq. (6) describes high-frequency beat motion with the beat period

$$T_b = \frac{2\pi}{\Omega \times (1 - \beta)}. \tag{7}$$

Note that the beat period is usually defined as the time between two successive beat amplitude maxima. It is not so evident from Fig. 1 that the high-frequency ion oscillation has in fact a nonsinusoidal form. It has a strong first harmonic at frequency $\Omega/2$, but higher harmonics $(n + 1)\Omega/2$ are also present, as can be seen from Eq. (6).

3. Beat-envelope equation method

3.1. Equation of the beat envelope

Consider the case of octopole-only imperfections. The equation of ion motion, Eq. (3), becomes

$$\frac{d^2u}{d\xi^2} + 2q\cos(2\xi) \times u = -q\cos(2\xi) \times 4\alpha_4 u^3. \tag{8}$$

The q parameter is close to that of the stability boundary q_0, hence the difference $q_0 - q$ is small. Eq. (8) may be expressed as

$$\frac{d^2u}{d\xi^2} + 2q_0\cos(2\xi) \times u = 2(q_0 - q)\cos(2\xi) \times u - q\cos(2\xi) \times 4\alpha_4 u^3. \tag{9}$$

The terms on the right side of Eq. (9) are small because $q - q_0$ and α_4 are small.

The solutions of Eq. (9) in case of a pure quadrupole ($\alpha_4 = 0$) are Mathieu functions. At the boundary of the first stable region ($q = q_0$), Eq. (9) has two independent solutions $u_1(\xi)$ and $u_2(\xi)$ that are presented in Fig. 2. The two solutions $u_1(\xi)$ and $u_2(\xi)$ in Fig. 2 are calculated for one RF period only. When calculated for a number of periods, the solution $u_1(\xi)$ shows periodic behavior, while the second solution $u_2(\xi)$ exhibits unstable motion with a linearly increasing amplitude of oscillation (Fig. 2b). Asymptotic behavior of the unstable solution may be expressed as follows: $u_2(\xi) \propto \xi u_1(\xi)$. This linear increase is specific to the boundary of stable region. In the unstable area, both solutions will have exponentially increasing amplitudes for the case of the linear Mathieu equation. However, for the case of the nonlinear Eq. (9), the ion motion goes out of resonance with the RF field because the vibration frequency depends on amplitude. The stability conditions are different. It is necessary to investigate carefully the structure of the periodic solution $u_1(\xi)$ for later use. The periodic solution may be derived from Eq. (9) with $\alpha_4 = 0$, $q = q_0$, and the initial

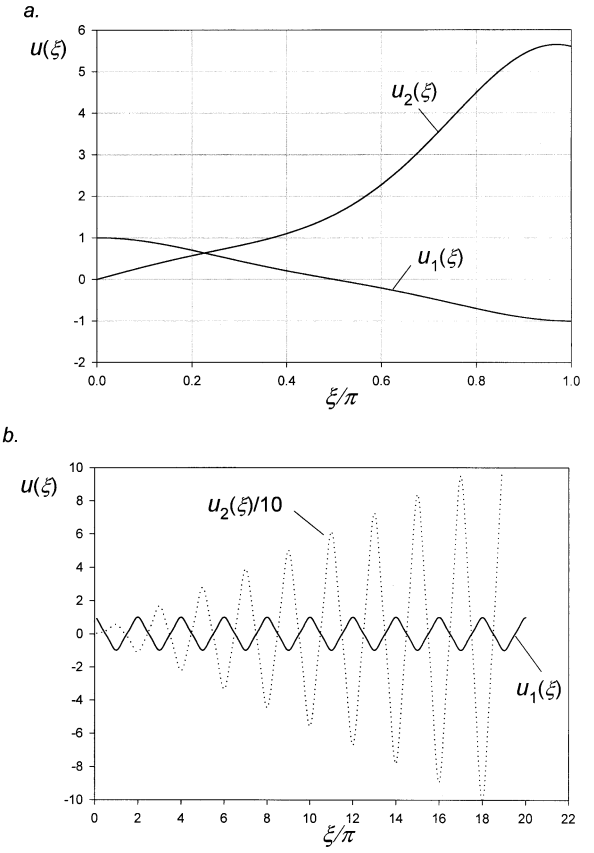

Fig. 2. Two particular solutions of the Mathieu equation with parameters at the boundary of stability: $a = 0$, $q = 0.908047$. The initial conditions are $u_1(0) = 1$, $u_1'(0) = 0$, $u_2(0) = 0$, $u_2'(0) = 1$. (**a**) Solutions are calculated for one RF period. (**b**) Solutions are calculated for longer scale.

conditions $u_1(\xi) = 1$, $u_1'(\xi) = 0$. It can be expressed in a Fourier series as follows:

$$u_1(\xi) = C_1 \times \cos(\xi) + C_3 \times \cos(3\xi) + C_5 \times \cos(5\xi) + \ldots. \tag{10}$$

The calculation of C_k is a well-defined procedure [14] and can be carried out with any prescribed accuracy: $C_1 = 0.904965$, $C_3 = 0.09164$, $C_5 = 0.003331$, $C_7 = 0.000062$. The solution $u_1(\xi)$ defines the form of the ion oscillations near the boundary.

Consider Eq. (9) with a q parameter different from q_0 and with field imperfections present. The solution may be expressed as follows:

$$u(\xi) = Z(\xi) \times u_1(\xi) + h(\xi) \times \sin(\xi) \quad (11)$$

Here, $Z(\xi)$ is a beat envelope, $u_1(\xi)$ describes the form of ion high-frequency oscillations, and $h(\xi)$ is an amplitude of oscillations 90° out of phase with the RF. Eq. (11) takes into account both solution $u_1(\xi)$ and $u_2(\xi)$ because the second solution may be expressed in terms of $u_1(\xi)$ with slowly varying amplitude. In the case of the linear Mathieu equation at the boundary ($q = q_0$), Eq. (11) gives a periodic solution, $Au_1(\xi)$, while $Z(\xi) = A = \text{const}$ and $h(\xi) = 0$. In the case of Eq. (8), the envelope function $Z(\xi)$ is not constant and $h(\xi) \neq 0$. However, if nonlinearity is weak and $|q_0 - q| \ll q_0$, the changes in these functions are small during each RF period.

Now we are going to use two approximate methods for the solution of the differential equation. The first is a perturbation technique [15] to take into account the terms on the right side of Eq. (9). Before applying perturbation methods, it is necessary to order the nonlinearity and the shift from the boundary and in such a way that their effects appear simultaneously in the same perturbation scheme. If we let $u(\xi) = \epsilon Z(\xi) \times u_1(\xi) + \epsilon^2 h(\xi) \times \sin(\xi)$, it is necessary to order the shift from the boundary as $\epsilon^2(q_0 - q)$. Here, ϵ is a small dimensionless parameter. It is introduced into the above equation as a book-keeping device and will be set to unity in the final solution. This ordering scheme is valid for the region close to the stability boundary. Eq. (8) then becomes

$$\begin{aligned} Z'' \times u_1 + 2Z' \times u_1' + \epsilon h'' \sin\xi + 2\epsilon h' \times \cos\xi \\ - \epsilon h \times \sin(\xi) + 2q_0 \epsilon h \times \sin\xi \cos 2\xi \\ = 2\epsilon^2(q_0 - q)(Z \times u_1 + \epsilon h \sin\xi) \cos 2\xi \\ - q \cos(2\xi) \times 4\alpha_4 \epsilon^2 (Z \times u_1 + \epsilon h \sin\xi)^3 \end{aligned} \quad (12)$$

The second approximation is the asymptotic method of slowly varying amplitudes [16]. This implies that the functions $Z(\xi)$ and $h(\xi)$ are very slow compared to cos (ξ), sin (ξ), and higher temporal harmonics. Harmonics cos (ξ), sin (ξ), and higher are present in Eq. (12) and have slowly varying amplitudes. One must set these amplitudes to zero to derive the equations for the slow functions $Z(\xi)$ and $h(\xi)$. Keeping the terms not higher than second order in ϵ gives the following equations (here we set $\epsilon = 1$):

$$C_1 \times Z'' + 2h' = (q_0 - q)(C_1 + C_3) \times Z - 4q\alpha_4 \Gamma_1 \times Z^3 \quad (13)$$

$$h'' - (1 + q_0) \times h = 2C_1 \times Z'. \quad (14)$$

Here, $\Gamma_1 = 0.46245$ is the first Fourier harmonic amplitude of the function $u_1^3 \cos(2\xi)$:

$$\Gamma_1 = \frac{2}{\pi} \times \int_0^{\pi} u_1^3(\xi) \cos(2\xi) \times \cos(\xi)\, d\xi. \quad (15)$$

Eq. (14) describes the damped and forced motion. The function $h(\xi)$ follows the slow function in the right part of Eq. (14). The approximate solution to this equation is the following:

$$h(\xi) = -\frac{2C_1}{1 + q} \cdot \frac{dZ}{d\xi}. \quad (16)$$

According to Eq. (16), $h(\xi)$ is small because it is proportional to the derivative of the slowly varying function $Z(\xi)$. This was assumed previously. From Eq. (13), one can derive the equation of the beat envelope as follows:

$$\frac{d^2Z}{d\xi^2} + 2J_2(q_0 - q) \times Z - 4\alpha_4 J_4 \times Z^3 = 0. \quad (17)$$

Here,

$$J_2 = \frac{C_1 + C_3}{2C_1} \cdot \frac{1 + q}{3 - q} = 0.502226,$$

$$J_4 = \frac{\Gamma_1}{C_1} \cdot \frac{q(1 + q)}{(3 - q)} = 0.423231.$$

Eq. (17) is like a Newton equation of motion for a particle in a potential field. A more accurate, but more complicated derivation, which takes into account the full series of higher temporal harmonics, is presented in Appendix A. This method and a different method that is based on a nonlinear transition matrix [17], both give values of J_2 and J_4, that are 13% smaller:

$J_2 = 0.438647$, $J_4 = 0.364295$. Eq. (17) is the Duffing equation. It is possible to derive the analytical solution [18] of this equation by means of elliptic integrals. In the case of a buffer gas, a damping force will be present in Eq. (17). With an RF voltage ramp, the coefficients in Eq. (17) become time dependent. With all this, it is not possible to solve Eq. (17) analytically.

3.2. Dispersion curve

Consider the beat-envelope equation that arises from Eq. (17) in the absence of nonlinear field imperfections. This gives the true value of the stability boundary, as follows. The envelope amplitude $Z(\xi)$ increases exponentially if $q > q_0$. In the opposite case, the beat envelope obeys the equation of harmonic motion with the frequency (dimensionless units)

$$\omega_b = \sqrt{2J_2(q_0 - q)}. \tag{18}$$

Eq. (18) contains the relation between the parameters β and q. According to the solution of the Mathieu equation, the beat frequency in dimensionless units equals $\omega_b = 1 - \beta$ (see Eq. [6]). From Eq. (18), we can derive the following equation:

$$q(\beta) = q_0 - \frac{1}{2J_2} \times (1 - \beta)^2$$

$$= 0.908047 - 1.39869 \times (1 - \beta)^2 \tag{19}$$

The dependence $\beta(q)$ may be calculated from the Mathieu equation directly. The result of this calculation is presented in Fig. 3. It is evident from this picture that Eq. (19) approximates the true dependence $q(\beta)$ near the point $\beta = 1$. Hence, the beat-envelope equation gives the correct Taylor series expansion of the curve $q(\beta)$ near the point $\beta = 1$.

3.3. Effective potential

Consider the envelope equation with the general higher field imperfections. In the case of hexapole imperfections, a constant term and an oscillation with the same frequency as the RF appear in the ion frequency spectrum. These have small amplitudes if β is close to 1 and if the hexapole field imperfection is small. An approach similar to that based on Eq. (8) is presented in Appendix B. It gives the same envelope equation as Eq. (17). The nonlinear constant is proportional to α_3^2 and is negative. If octopole and hexapole fields are present, ion motion may be described by the beat-envelope Eq. (17) with a nonlinear constant that takes into account the hexapole imperfections:

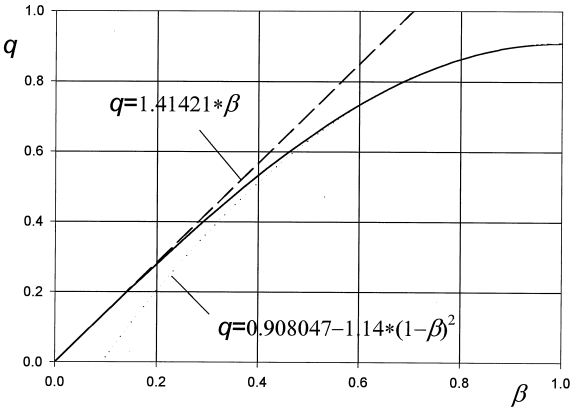

Fig. 3. Dispersion curve of the axial oscillations in the RF regime. The solid curve is from the solution of the Mathieu equation. Dashed lines are the result of the secular motion equation (near $\beta = 0$) and of the beat-envelope equation (near $\beta = 1$).

$$\alpha_4^* = \alpha_4 - 7.9091 \times \alpha_3^2. \tag{20}$$

It follows from this equation that the influence of a hexapole imperfection is similar to the influence of a negative octopole field.

In the case of a general field imperfection of even-order $2N$, the envelope equation will have a nonlinear force that is proportional to $\alpha_{2N-1} Z^{2N-1}$. Odd-field imperfections of the order $2N - 1$ will contribute to the same force, but this contribution will be negative: $-\alpha_{2N-1}^2 Z^{2N-1}$. The envelope equation will be like a Newton equation of a particle motion in the potential field:

$$U_{eff}^{(b)}(Z) = J_2(q_0 - q) \times Z^2 - J_4 \alpha_4^* \times Z^4 - J_6 \alpha_6^* \times Z^6 - \ldots . \tag{21}$$

Here, α_N^* is the amplitude of a higher even-order field, which is corrected to take into account the influence of lower order odd fields. The trapping efficiency depends on the behavior of this potential function at the boundary. Consider the negative field composition if $U_{eff}^{(b)}(Z)|_{q=q_0}$ is a potential well. The ion motion is stable in general even if $q > q_0$. The positive field composition takes place if $U_{eff}^{(b)}(Z)|_{q=q_0}$ is a potential hill. In this case, the ion motion is stable only if $q < q_0$. It follows that the conditions for the stability of ion motion are different from the case of a linear Mathieu equation. For simplicity, the value q_0 will be called the boundary in the discussion below. Consequently, the unstable area means $q > q_0$, as described previously.

The potential function with octopole-only imperfections is presented in Fig. 4. In the case of a positive octopole field (Fig. 4a), there is a potential well within the stable area. The width and depth of the well decrease if q approaches the boundary. In the case of a negative octopole field, there is a confining potential not only in the stable area but also in the unstable region. In the unstable area, the potential function becomes a double well (Fig. 4b).

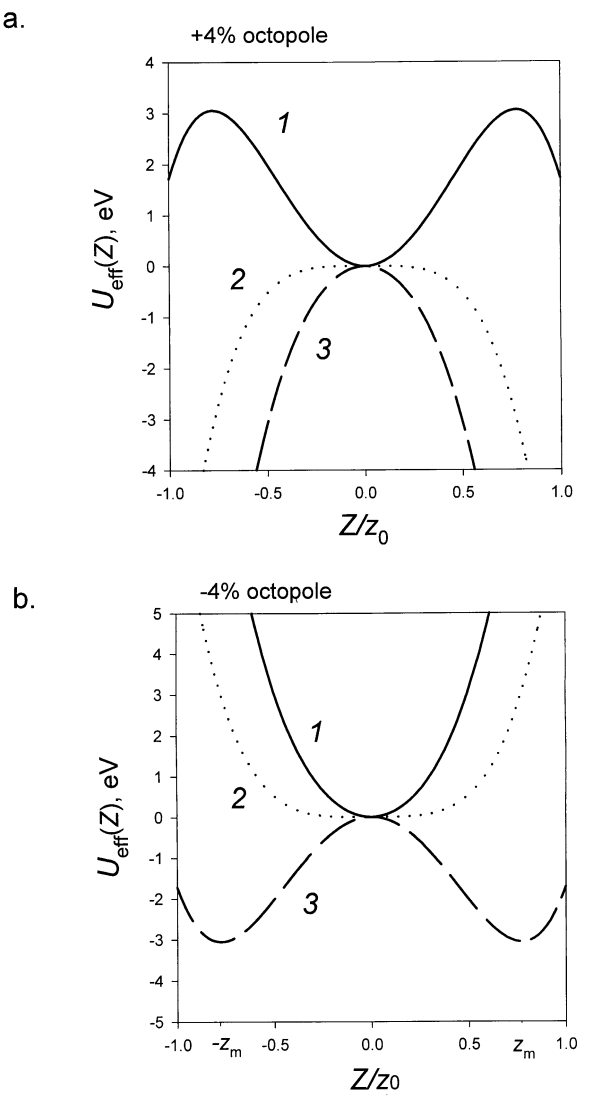

Fig. 4. Potential function of the beat envelope equation. Parameters are calculated for an ion mass $M = 100$ Da in a typical ion trap. Line 1 is for the stable region: $q = 0.868$. Line 2 is at the boundary: $q = 0.908$. Line 3 is for the unstable region: $q = 0.948$.

4. Results of the beat-envelope equation

4.1. Ejection delay caused by a negative octopole field

The Paul ion trap with truncated electrodes shows poor mass resolution in a mass-selective axial instability scan [19]. The truncation of the hyperbolic electrodes gives rise to higher field imperfections, the strongest of which is the octopole [5]. The sign of the octopole field is opposite to that of the basic quadrupole field. This negative octopole field is regarded [20] as responsible for the poor mass resolution of the truncated Paul trap.

Consider the envelope equation, Eq. (17), with a negative octopole field. The quadratic part of the potential function Eq. (21) equals zero at the boundary. Consequently, there is a band of q values near the boundary for which the stability of ion motion is governed by higher fields. In the case of a negative octopole field, $\alpha_4^* < 0$ and the potential function is confining. It has the form of the usual well inside the stable region and becomes a double well in the unstable region (Fig. 4b). The potential function has two minima at the points

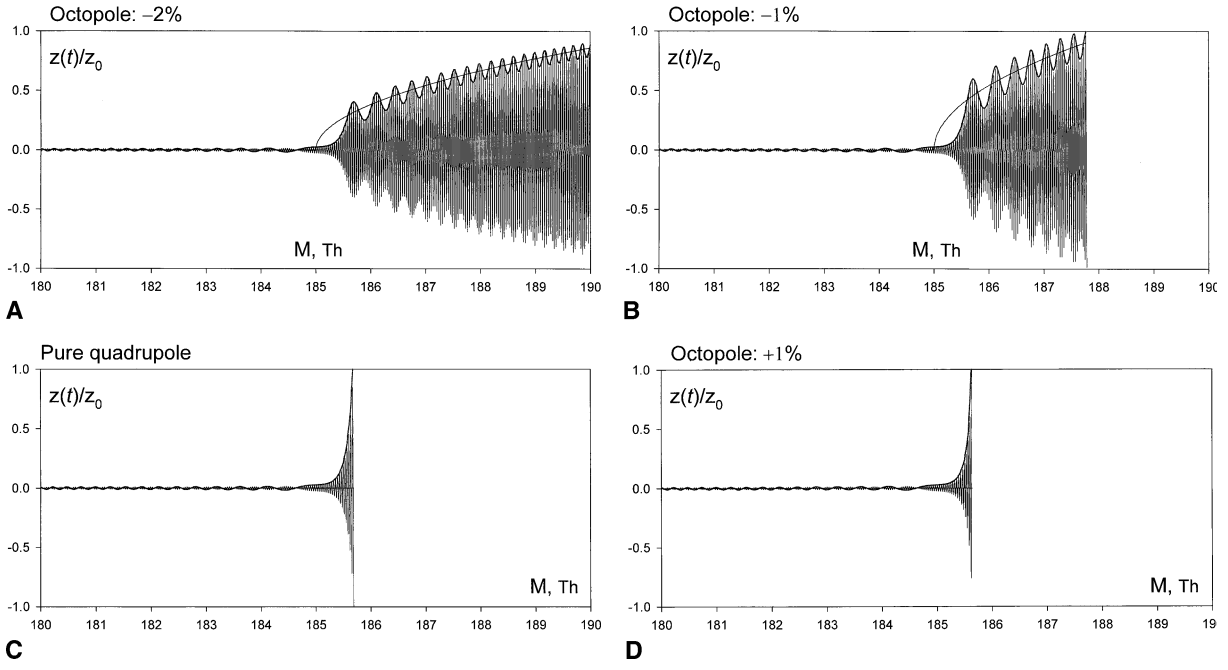

Fig. 5. Simulated axial oscillation of mass 185 Th in a scan range 180–190 Th. Wide solid lines on this graph are the solution of the envelope equation and the position of the potential well minimum (on **a** and **b** only).

$$z_m = \pm z_0 \times \sqrt{\frac{J_2(q_0 - q)}{2J_4\alpha_4^*}}. \quad (22)$$

Ions do not leave the trap until the potential minima are outside the ion trap's dimensions.

This is illustrated in Fig. 5, which shows the results of the numerical solutions of Eq. (3) for the case of boundary ejection. The calculation parameters correspond to the typical ion trap: field radius $r_0 = 10$ mm, RF frequency $\Omega = (2\pi) \times 1.04$ MHz. The RF amplitude V is ramped linearly in time. It defines the ion mass that meets the stability boundary at a given time. The mass scan speed is $\lambda = \mathrm{dM/d}t = 5555$Da/s, as is commonly used. In accordance with this, the time axis of Fig. 5 is scaled in mass units. The trajectories presented in Fig. 5 resemble those of [6]. The envelope of the trajectory, calculated from Eq. (17), almost coincides with the true envelope. It is evident from Fig. 5a and Fig. 5b that ions leave the trapping volume when the position of the potential minimum becomes $> z_0$. Hence, the ion ejection delay in a truncated Paul trap appears to be caused by the existence of the potential well in the unstable area. This takes place if the higher field harmonics are negative.

4.2. Potential well within the unstable area

In the case of a negative octopole field, the potential function has two symmetrically placed minima at $+z_m$ and $-z_m$. Collisional damping of the ion motion occurs in practice because of collisions with the helium buffer gas. This causes the beat envelope to go into equilibrium at one of the potential minima. In this state, the ion oscillates with half the frequency of the RF and with constant amplitude. In equilibrium, the ion gains energy from the field during the first period of RF, and it returns the same energy during the next period. This type of oscillation takes place in the unstable region only, and it is significantly nonlinear.

This prediction results from the envelope equation, which is approximate. Hence, it is useful to confirm

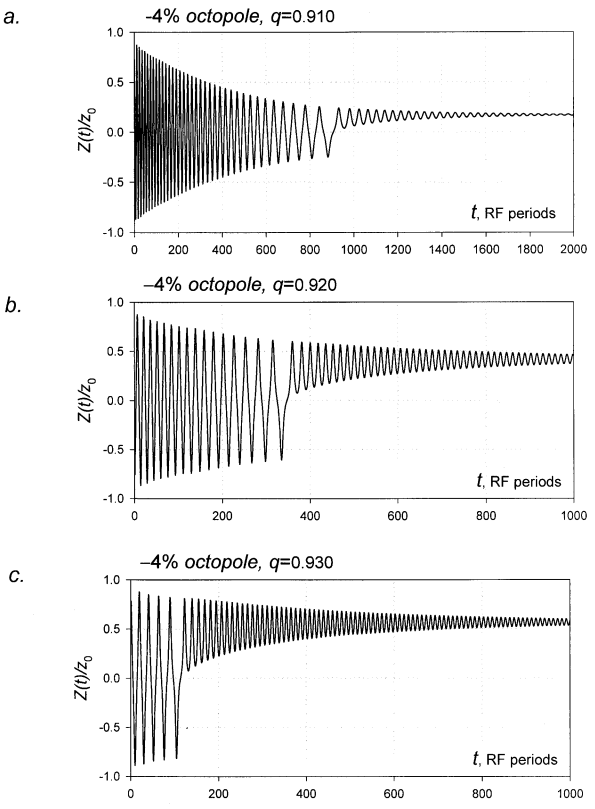

Fig. 6. Simulated ion axial oscillation for the case of a negative octopole field. The envelope only is presented. This is the numerical solution of Eq. (23) with −4% octopole field and a linear damping coefficient $\gamma = 0.005$.

this by direct numerical solution of the axis model. With linear damping and an octopole-only imperfection, Eq. (3) can be written as

$$\frac{d^2u}{d\xi^2} + 2\gamma\frac{du}{dt} + 2q\cos(2\xi) \times u = -q\cos(2\xi) \times 4\alpha_4 u^3. \quad (23)$$

Here, γ is a damping constant. The numerical solution of Eq. (23) over comparatively long times is shown in Fig. 6. The initial position of an ion is taken close to the trap dimensions. At first, the envelope shows nonlinear symmetric oscillations about the point $z = 0$. The amplitude of oscillation decreases because of damping. With time, the envelope becomes asymmetric and appears near the potential minimum at z_m. Finally, the envelope goes into equilibrium at this position. The potential function minimum position z_m, which can be derived from this numerical calculation, is in excellent agreement with Eq. (22).

The ion motion in the equilibrium state is correlated with the trapping field. With damping, the ion motion goes into this state independent of the initial conditions. Such motion in the theory of vibrations is called a "limit cycle" [16,21]. To describe the ion motion in a phase space (z, z'), it is useful to plot only one point at the beginning of each RF cycle. This description is named a Poincaré section. The Poincare' section of the ion motion in case of Fig. 6 is presented in Fig. 7. The cycle motion depends on the magnitude of the nonlinear field and is not very sensitive to its actual form because of structural flexibility of the limit cycle. After some time, all ions move coherently on the same limit cycle. This time depends on the damping constant, but it is not very critical which damping mechanism is present. This is also the case for the influence of axial–radial motion interactions. The radial motion will not have a significant influence on the axial limit cycle unless these motions are in resonance.

4.3. Depth of the potential well

The method of trajectory averaging or the secular-motion equation is frequently used to describe ion motion in an RF quadrupole field [10–12]. This method applies to the Mathieu equation at the beginning of the stability diagram where the parameters a and q have small values in order that $\beta \ll 1$. Ion oscillation in this case has the form of a slow oscillation with comparatively small-amplitude fast oscillations at the RF frequency superimposed:

$$u(\xi) = Z(\xi) + h(\xi) \times \cos 2\xi. \quad (24)$$

The secular motion $Z(\xi)$ obeys the equation of harmonic oscillation:

$$\frac{d^2Z}{d\xi^2} + \left(a + \frac{q^2}{2}\right) \times Z = 0. \quad (25)$$

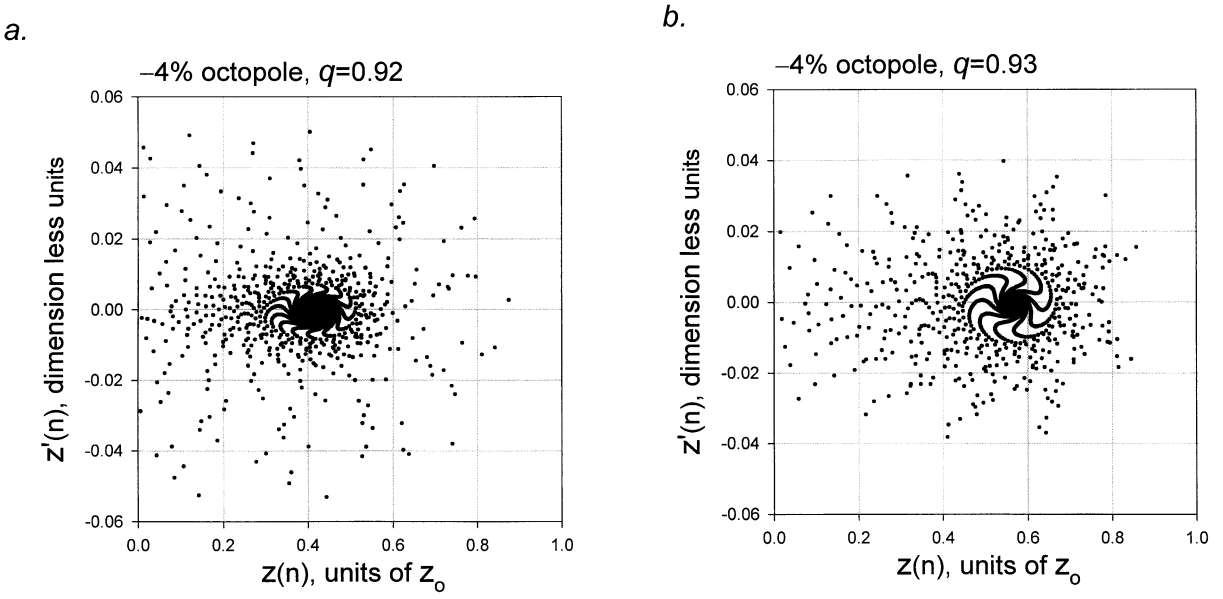

Fig. 7. Poincare section of the ion axial phase space. The ion velocity is expressed in the units of $r_0\Omega/2$. Initial conditions and parameters of (**a**) the same as in Fig. 6b, and of (**b**) the same as in Fig. 6c.

Eq. 25 defines the lower boundary of the first stable region: $a = -0.5q^2$. Within the stable region, the secular oscillations have a frequency ω_s given by

$$\omega_s = \frac{\Omega\beta}{2}; \qquad \beta = \sqrt{a + 0.5q^2}. \tag{26}$$

Harmonic oscillation of an ion, as described by Eq. (25), takes place in a quadratic potential. Consequently, the effective potential function of the secular motion can be written as

$$U_{eff}^{(s)}(Z) = \left(a + \frac{q^2}{2}\right) \times \frac{Z^2}{2} = \beta^2 \times \frac{Z^2}{2}. \tag{27}$$

The potential well of Eq. (27) has infinite depth, but the ion motion is confined within the limits of the ion trap: $|Z| < z_0$. With these assumptions, we derive the well depth D_z:

$$D_z = \frac{M\Omega^2}{4e} \times U_{eff}^{(s)}(z_0) = \frac{M\Omega^2 z_0^2}{4e} \cdot \frac{\beta^2}{2}. \tag{28}$$

The depth of the potential well D_z has a physical meaning of the energy that an ion must acquire to leave the trapping volume.

The effective potential well depth was proposed by Dehmelt and is valid if a and q are small. It is widely used in practical mass spectrometry [22,23]. In the case of ion motion with a q parameter close to the boundary $q_0 = 0.908047$, this method is not applicable. However, it is evident from the equation of the beat envelope that a potential well exists in this case too. According to Eq. (21), the potential function of a pure quadrupole field is quadratic. Hence, the depth of the potential well can be defined similar to the Dehmelt case:

$$\begin{aligned} D_z &= \frac{M\Omega^2}{4e} \times U_{eff}^{(b)}(z_0) \\ &= \frac{M\Omega^2 z_0^2}{4e} J_2(q_0 - q) \\ &= \frac{M\Omega^2 z_0^2}{4e} \times \frac{(1-\beta)^2}{2}. \end{aligned} \tag{29}$$

This equation follows from the beat-envelope equation and is valid near the $\beta_z = 1$ boundary. A plot of the potential well depth D_z versus q is presented in

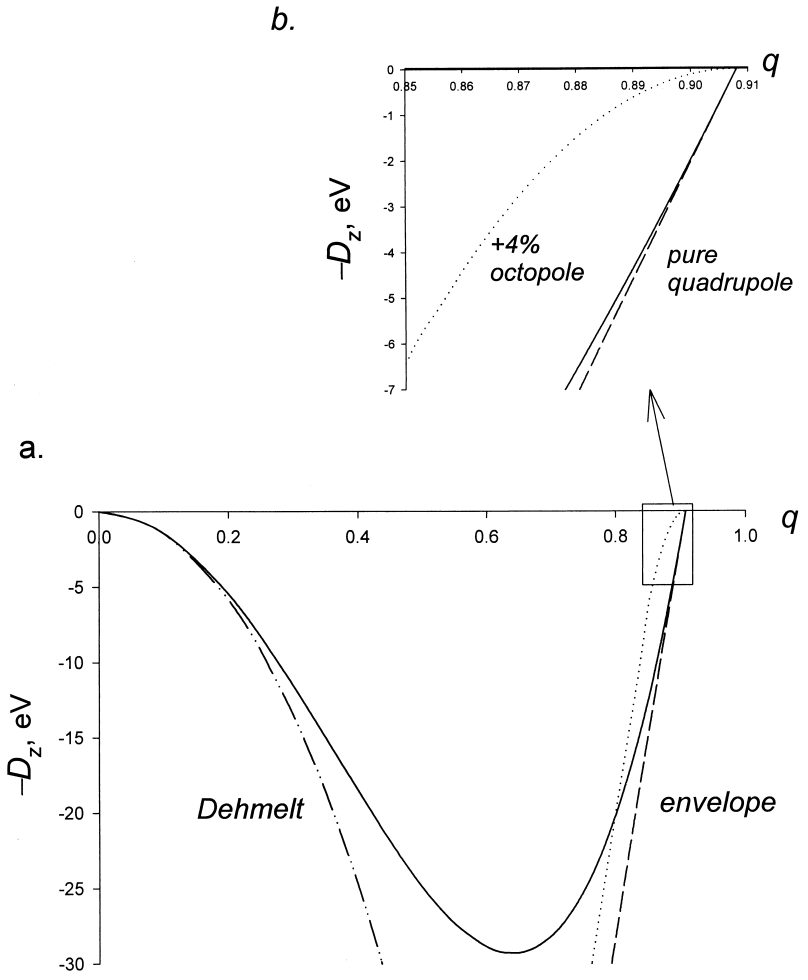

Fig. 8. Potential well depth in the RF only regime for 100-Da ions as a function of q. (**a**) A sample curve of the trapping well depth for entire first stable. (**b**) Detailed picture near the boundary.

Fig. 7. Both the Dehmelt and the beat-envelope cases are presented in this figure. The well depth for the entire first stability region is given by the solid line. It is similar to the curve given by R. March in the discussion of resonant ejection and without derivation in the tutorial paper [24].

It follows from the Eq. (29) that the potential well depth is proportional to the first power of $q_0 - q$. If a positive octopole field is present, the potential function is not quadratic, and it has the form of a symmetric well of finite depth and width (Fig. 4a). The well width with a negative octopole is twice the value given by Eq. (22). It is not equal to the trap dimensions, and it decreases as q approaches the stability boundary. As a result, the potential well depth decreases as the second power of $q_0 - q$:

$$D_z = \frac{M\Omega^2}{4e} \times U_{eff}^{(b)}(z_m) = \frac{M\Omega^2 z_0^2}{4e} \times \frac{J_2^2}{4J_4\alpha_4}(q_0 - q)^2, \quad \text{if} \quad z_m < z_0; \tag{30}$$

$$D_z = \frac{M\Omega^2}{4e} \times U_{eff}^{(b)}(z_0)$$

$$= \frac{M\Omega^2 z_0^2}{4e} \times [J_2(q_0 - q) - J_4\alpha_4],$$

$$\text{if} \quad z_m > z_0. \tag{31}$$

This means, in practice, that the trapping volume is cleared more rapidly as the working point q approaches the boundary. This appears to be because of the influence of the positive-octopole field. A detailed plot of the $D_z(q)$ dependence near the boundary, with and without an octopole term, is presented in Fig. 8b.

5. Discussion

Weak higher-field imperfections are known to have a surprisingly strong influence on the operation of quadrupole ion traps. Discussion of the ion motion in an RF quadrupole field with weak multipole fields is important for practical mass spectrometry and ion trapping. In the past, the analytical approach to this problem has been limited to the secular motion equation. This equation is valid if the value of stability parameter β is small. In most of the mass-spectrometric operation protocols, the ions meet the boundaries of the stable region. The equation of averaged motion is not applicable in this case. However, the ion motion with parameters close to the boundaries of stability always has slow variables. It is possible to derive the equations for the slow variables within the framework of perturbation theory.

This approach to calculating the ion motion, with parameters close to the boundary $\beta_z = 1$, is shown in this article. The slow variable in this case is the ion beat envelope. The ion oscillation has a frequency of half the trapping RF and a nonsinusoidal form that is governed by the periodic solution $u_1(\xi)$ of the Mathieu equation at the boundary. If this is taken into account, the equations of slow variables give the true value to the boundary of stable region and the dispersion curve $\beta(q)$.

The equation of the beat envelope reveals the influence of higher fields on the ion motion. The odd higher fields are averaged in the first order, but they contribute in the second order. This contribution is proportional to the second power of the field amplitude and does not depend on its sign. The influence of odd fields is similar to the influence of negative even fields. The even higher fields contribute in the first order, and their influence strongly depends on their sign. In the case of positive field contributions, the potential well of the beat-envelope motion exists inside the stable area and disappears at the boundary. The depth of the potential well decreases as q approaches the boundary and disappears in the unstable area. In the case of negative field contributions, the ion motion is stable in general. The potential function has a double well in the unstable area. There is a band of q values near the boundary for which the minima of the effective potential function are placed inside the trapping volume. This is confirmed by the direct numerical solution of the Mathieu equation with weak nonlinearity and damping. Ions strike the electrodes if the minima move outside the trapping volume. This explains the destructive influence of the negative higher field composition on a boundary mass selective axial instability ejection in a Paul trap with truncated hyperbolic electrodes.

The ion ejection delay also increases the chemical mass shift [8,9]. With the help of the envelope equation, it is possible to describe the process of ion ejection in detail. This requires information about the electric field inside the real ion trap, which depends strongly on the electrode geometry. In any case, the numerical solution of the envelope equation is much easier than the solution of original equation of the ion motion with the high-frequency trapping field.

The potential well depth is calculated as a function of q. In the case of a pure quadrupole field, the well depth is proportional to first power of $q_0 - q$; if a positive octopole field is present, it is proportional to the second power of $q_0 - q$. These lead to more rapid ejection of ions from the trapping volume in a mass-selective axial instability scan. Therefore, higher mass resolution is achieved in nonlinear ion traps, such as the stretched ion trap and the modified hyperbolic angle trap.

The influence of small field imperfections on RF

quadrupole devices operation is surprisingly strong. Almost all of these devices use the ion motion with parameters close to the boundaries of the stability region. If we describe the ion motion by an effective potential, a trapping potential well must exist everywhere inside the stable area. The trapping efficiency of the quadrupole RF field goes to zero at the boundary of the stability region. Consequently, the ion motion near the boundary is dominated by the higher field imperfections regardless of how small they are compared to the quadrupole field. The above treatment does not take into account ion motion in the radial direction. For a more realistic ion motion description, the ion–ion Coulomb interactions and the effect of the trapping voltage ramping must be properly included in the equations. The linear damping model is also too simplified for the descriptions of the ion collisions with buffer gas.

Accurate investigation shows that ion–neutral collisions, when the ion speed is significantly greater than the thermal speed of the gas, lead, in fact, to quadratic damping [25,26]. Ion–neutral collisions have the character of discrete events, as the interaction time is small compared with the RF period. Thus, the model used in this article is not applicable to the description of the motion of one particular ion. Nevertheless, it is valid for the description of an ensemble of identical ions. This means that a more detailed simulation of the ion motion by means of the Monte-Carlo method, being repeated with the same ion initial conditions, will give the averaged motion described by dynamical Eq. (23). In practice, such averaging of the ion trajectories appears because of the large number of trapped ions, which move independently in the case of sufficiently low ion density. It should be noted that all discussion of damping in this article is for the case of a small mass of the buffer gas compared with the ion mass. In this case, the ion speed after a collision does not change significantly in direction. In each collision, the energy of the ion is decreased by a small amount, depending on $m_{\text{buffer}}/m_{\text{ion}}$. If this condition is not valid, then a big phase shift between the ion motion and RF field appears after each collision. Hence, cooling of the ions to the limit cycle, as shown in Fig. 6, will not occur to a significant extent.

The envelope equation reveals the main trend of the influence of higher fields on a ion ejection at the boundary. This is related to the qualitative changes in the ion-motion stability conditions. The linear Mathieu equations of the ion motion have limited region of validity even in the case of a small nonlinearity. The ion motion near the boundary of stability is very sensitive to all kinds of imperfections. When the linear motion is unstable, stability may be achieved by means of nonlinear fields. The coherent cycle motion of ions is also possible.

6. Acknowledgements

Author is grateful to N.V. Konenkov and A.E. Romanov for fruitful discussion of this work. Author also gratefully acknowledge Don J. Douglas for his invitation to spend a month in his laboratory in the University of British Columbia, which gave me an opportunity to finish this work.

Appendix A: envelope equation with an octopole field with the full series of harmonics

In the case when an octopole field is present, the ion axial motion equation is Eq. (8). If the full series of harmonics is taken into account, the solution can be written as

$$u(\xi) = \epsilon \times Z \times u_1(\xi) + \epsilon^2(h_1 \sin \xi + h_3 \sin 3\xi + h_5 \sin 5\xi + \dots) + \epsilon^3(g_3 \cos 3\xi + g_5 \cos 5\xi + \dots). \quad \text{(A1)}$$

Here, $Z(\xi)$ is the beat envelope, and $h_k(\xi)$ and $g_k(\xi)$ are the slowly varying amplitudes of the cos and sin overtones. The cosine series begins with g_3 because the first harmonic amplitude g_1 is the function of interest, $Z(\xi)$. The beat envelope is considered to be a slowly varying function compared to cos ξ, sin ξ, and higher temporal harmonics. The value $q_0 - q$ is of the second order $\sim\epsilon^2$. Functions h_k are of the first and g_k are of the second order, as will be proved later. To

derive the equations of the slow variables, one must substitute Eq. (A1) into Eq. (8) and keep the terms not higher than second order in ϵ. All derivatives of g_k, and the second derivatives of h_k, may be neglected in this approximation because of their slow behavior. Eq. (8) can be written as

$$\begin{aligned} Z''u_1 + 2Z'u_1' + 2\epsilon h_1' \cos\xi - \epsilon h_1 \sin\xi \\ + 6\epsilon h_3' \cos 3\xi - 9\epsilon h_3 \sin 3\xi + \ \ldots \\ - 9\epsilon^2 g_3 \cos 3\xi - 16\epsilon^2 g_5 \cos 5\xi - \ \ldots \\ + 2q \cos 2\xi \times [\epsilon h_1 \sin\xi + \epsilon h_3 \sin 3\xi \\ + \epsilon^2 g_3 \cos 3\xi + \ldots] \\ = -2\epsilon^2(q - q_0) \cos 2\xi \times u_1 Z - \epsilon^2 q \cos 2\xi \\ \times 4\alpha_4 u_1^3 Z^3. \end{aligned} \tag{A2}$$

The usual procedure of averaging requires the amplitudes of all harmonics in Eq. (A2) to be equal to zero. The averaging of cos $K\xi$ ($K = 1, 2, 3, \ldots$) gives the following system of equations (ϵ is set to unity):

$$\begin{aligned} C_1 Z'' + 2h_1' + qg_3 = -(q - q_0)(C_1 + C_3)Z \\ - 4q\alpha_4 D_1 \times Z^3, \\ C_3 Z'' + 6h_3' - 9g_3 + qg_5 = -(q - q_0)(C_1 \\ + C_5)Z - 4q\alpha_4 D_3 \times Z^3, \\ C_5 Z'' + 10h_5' - 25g_5 + q(g_3 + g_5) = -(q \\ - q_0)(C_3 + C_7)Z - 4q\alpha_4 D_5 \\ \times Z^3 \ldots . \end{aligned} \tag{A3}$$

Here, C_K are the Fourier harmonics of the function u_1 and D_K are the Fourier harmonics of the function u_1^3 cos 2ξ. Calculation gives $D_1 = 0.46245$, $D_3 = 0.34508$, $D_5 = 0.15457$, $D_7 = 0.03341$, and $D_9 = 0.00414$. Averaging of sin $K\xi$ gives the second system of equations:

$$\begin{aligned} -2C_1 Z' - h_1 + q(h_3 - h_1) = 0, \\ -6C_3 Z' - 9h_3 + q(h_5 + h_1) = 0, \\ -10C_5 Z' - 25h_5 + q(h_7 + h_3) = 0 \ldots . \end{aligned} \tag{A4}$$

The solution to the system of equations, Eq. (A4), may be expressed as $h_k = -\sigma_k Z'$ ($k = 1, 2, 3, \ldots$), where σ_k are unknown numbers. From the system (A4), we derive a chain of equations for σ_k as follows:

$$\begin{aligned} \sigma_1 - q(\sigma_3 - \sigma_1) = 2C_1, \\ 9\sigma_3 - q(\sigma_5 + \sigma_1) = 6C_3, \\ 25\sigma_5 - q(\sigma_7 + \sigma_3) = 10C_5, \ldots . \end{aligned} \tag{A5}$$

Each number $\sigma_3, \sigma_5, \ldots$ is expressed by σ_1 and consequently eliminated from this system. As a result, we derive the equation to define σ_1 and values of all σ_k. With this method, for the case where $q = q_0$, we calculate the following: $\sigma_1 = 1.02733$, $\sigma_3 = 0.16549$, $\sigma_5 = 0.00735$, $\sigma_7 = 0.000154$, and $\sigma_9 = 0.0000019$.

The solution of the system (A4), if substituted into the system (A3), leads to the infinite system of equations for the unknown functions g_k. The solution method is the same as used previously. The functions $g_3, g_5, \ldots$ are expressed via the envelope function $Z(\xi)$. On eliminating these functions from the system, one will derive an equation for the envelope function $Z(\xi)$. This equation is Eq. (17). Calculation gives the values $J_2 = 0.43865$ and $J_4 = 0.36429$. From the solution of the systems (A3) and (A4), it is evident that the functions h_k and g_k are of the first and second orders, as was previously assumed.

Appendix B: hexapole and higher fields in the beat-envelope equation

The equation of ion axial motion in the case of an added hexapole field can be written as

$$u'' + 2q \cos 2\xi \times u = -q \cos 2\xi \times 3\alpha_3 u^2. \tag{B1}$$

The nonlinear term is quadratic in u. Because of this, the zero term $g_0(\xi)$ and other even harmonics appear in the ion oscillations in addition to the terms that are present in Eq. (A1). The solution in this case can be written as

$$z(\xi) = \epsilon Z \times u_1(\xi) + \epsilon^2(h_1 \sin \xi + h_2 \sin 2\xi + h_3 \sin 3\xi + \dots) + \epsilon^3(g_0 + g_2 \cos 2\xi + g_3 \cos 3\xi + \dots). \quad \text{(B2)}$$

As previously, we consider $q - q_0$ as a second-order value. In the second order, the nonlinear part of Eq. (B1) is calculated to be

$$\alpha_3 z^2 \approx \epsilon^2 \alpha_3 u_1^2 \times Z^2 + 2\epsilon^3 \alpha_3 u_1 Z(h_1 \sin \xi + h_2 \sin 2\xi + \dots + \epsilon g_0 + \epsilon g_2 \cos 2\xi + \dots). \quad \text{(B3)}$$

Substituting Eq. (B3) into Eq. (B1) gives the infinite system of equations for higher harmonic amplitudes. We present this system in parts. First, the even sine harmonics give the system of equations:

$$\begin{aligned} -4h_2 + qh_4 &= 0, \\ -16h_4 + q(h_6 + h_2) &= 0, \\ -36h_6 + q(h_8 + h_4) &= 0 \dots . \end{aligned} \quad \text{(B4)}$$

This system has a trivial solution. Consequently, the amplitudes of the even sine harmonics h_{2k} are, in fact, the small values of the third order. The odd sine harmonics satisfy the system (A4), which was solved previously (Appendix A): $h_k = -\sigma_k Z'$, $k = 1, 3, 5, \dots$.

The even cosine harmonics give the following system of equations:

$$\begin{aligned} qg_2 &= -3q\alpha_3 G_0 \times Z^2, \\ -4g_2 + q(2g_0 + g_4) &= -3q\alpha_3 G_2 \times Z^2, \\ -16g_4 + q(g_2 + g_6) &= -3q\alpha_3 G_4 \times Z^2 \dots . \end{aligned} \quad \text{(B5)}$$

Here, G_K are the Fourier harmonic amplitudes of the function $u_1^2 \cos 2\xi$. Calculation gives $G_0 = 0.49272$, $G_2 = 0.34508$, $G_4 = 0.24999$, $G_6 = 0.04316$, and $G_8 = 0.003641$. The solution of this system can be written as $g_{2k} = -3q\alpha_3 \Delta_{2k} Z^2$. The infinite system of equations for the unknown numbers Δ_{2k} arises from the system (B5). It is solved by the same method, which was described previously. We find for $q = q_0$ the following values: $\Delta_0 = 1.30669$, $\Delta_2 = 0.49272$, $\Delta_4 = 0.01373$, $\Delta_6 = -0.00074$, and $\Delta_8 = -0.00006$.

The equation of the beat envelope arises from the system for the odd cosine harmonic amplitudes:

$$\begin{aligned} C_1 Z'' + (q - q_0)(C_1 + C_3) + 2h_1' + qg_3 &= 18q^2\alpha_3^2 F_1 \times Z^3, \\ C_3 Z'' + (q - q_0)(C_1 + C_5) + 6h_3' - 9g_3 + qg_5 &= 18q^2\alpha_3^2 F_3 \times Z^3, \\ C_5 Z'' + (q - q_0)(C_3 + C_7) + 10h_5' - 25g_5 + q(g_3 + g_5) &= 18q^2\alpha_3^2 F_5 \times Z^3 \dots . \end{aligned} \quad \text{(B6)}$$

Here, F_{2k+1} are the Fourier harmonic amplitudes of the function

$$f(\xi) = u_1(\xi) \cos 2\xi \cdot (\Delta_0 + \Delta_2 \cos 2\xi + \Delta_4 \cos 4\xi + \dots).$$

The system (B6) is analogous to the system (A3). The functions $g_3, g_5, \dots$ are expressed by the envelope function. The functions $g_3, g_5, \dots$ are then eliminated from the system. Therefore, we derive the equation of the beat envelope. This calculation gives the following equation:

$$\frac{d^2Z}{d\xi^2} + 0.87729(q_0 - q) \times Z + 12.692\alpha_3^2 \times Z^3 = 0. \quad \text{(B7)}$$

This equation is the same as in the case of an octopole field (Eq. [17]). The nonlinear constant depends on the strength of hexapole field and is always negative. Both octopole and hexapole fields may be included in the nonlinear constant of the following equation:

$$\alpha_4^* = \alpha_4 - 7.9091 \times \alpha_3^2. \quad \text{(B8)}$$

With the result of Appendices A and B, we can speculate about the influence of higher fields on the

ion beat envelope. The even field $2N$ ($N = 2, 3, 4, \ldots$) gives a force that is proportional to $\alpha_{2N}Z^{2N-1}$. The odd field harmonic $2N - 1$ contributes to the same force. This contribution is negative $-\alpha_{2N-1}^2 Z^{2N-1}$. The true value of the nonlinear constant α_{2N}^* may be corrected to take into account contributions from lower-order fields. The resulting beat envelope equation will be like a Newton equation.

References

[1] G.C. Stafford Jr., P.E. Kelley, J.E.P. Syka, W.E. Reynolds, J.F.J. Todd, Int. J. Mass Spectrom. Ion Processes 60 (1984) 85.
[2] G.C. Stafford, P.E. Kelley, D.R. Stephens, U.S. Patent 4,540,884.
[3] The modified angle ion trap was developed by Bruker-Franzen Analytic GmbH, under contract DAAA15-87-C0008 awarded to Teledyne CME, for the US Army ERDEC (Aberdeen Proving Ground) as "Chemical-Biological Mass Spectrometer" CBMS.
[4] Y. Wang, J. Franzen, K.P. Wanczek, Int. J. Mass Spectrom. Ion Processes 124 (1993) 125.
[5] Y. Wang, J. Franzen, Int. J. Mass Spectrom. Ion Processes 132 (1994) 155.
[6] J. Franzen, Int. J. Mass Spectrom. Ion Processes 125 (1993) 165.
[7] J. Franzen, Int. J. Mass Spectrom. Ion Processes 130 (1994) 15.
[8] J.M. Wells, W.R. Plass, R.G. Cooks, Anal. Chem. 72 (2000) 2677.
[9] J.M. Wells, W.R. Plass, G.E. Patterson, Z. Ouyang, E.R. Badman, R.G. Cooks, Anal. Chem. 71 (1999) 3405.
[10] L.D. Landau, E.M. Lifshitz, Mechanics, Pergamon, Oxford, 1960.
[11] R.F. Wuerker, H. Shelton, R.V. Langmuir, J. Appl. Phys. 30 (1959) 342.
[12] H.G. Dehmelt, Adv. At. Mol. Phys. 3 (1967) 53.
[13] M. Sudakov, Russ. J. Tech. Phys. 70 (2000) 37.
[14] N.W. McLachlan, Theory and Applications of Mathieu Functions, Oxford University Press, Oxford, 1974.
[15] A.H. Nayfeh, Problems in Perturbation, Wiley, New York, 1985.
[16] N.N. Bogoliubow, Y.A. Mitropolsky, Asymptotic methods in the theory of nonlinear oscillations, Hindustan, Delhi, 1961.
[17] M. Sudakov, Russ. J. Tech. Phys. (submitted).
[18] A. Blaquere, Nonlinear System Analysis, Academic Press, New York, 1966.
[19] J. Louris, J. Schwartz, G. Stafford, J. Syka, D. Taylor, The Paul Ion Trap Mass Selective Instability Scan: Trap Geometry and Resolution, Proceedings of the Fortieth ASMS Conference on Mass Spectrometry and Allied Topics, Washington, DC, 1992.
[20] J. Franzen, R.-H. Gablign, M. Schubert, Y. Wang, in: J.F.J. Todd, R.E. March (Eds.), Practical Aspects of Ion Trap Mass Spectrometry, CRC Press, 1995 (Chapter 3).
[21] F.C. Moon, Chaotic Vibrations, Wiley, New York, 1987.
[22] J.F.J. Todd, G. Lawson, R.F. Bonner, in: P.H. Dawson (Ed.), Quadrupole Mass Spectrometry and Applications, Elsevier, 1976 (Chapter 8).
[23] R.E. March, R.J. Hughes, Quadrupole Storage Mass Spectrometry, Wiley.
[24] R.E. March, J. Mass Spectrom. 32 (1997) 351.
[25] D.J. Douglas, J. Am. Soc. Mass Spectrom. 5 (1994) 17.
[26] Yu-Luan Chen, B.A. Collings, D.J. Douglas, J. Am. Soc. Mass Spectrom. 8 (1997) 681.